Application of seismic tomography in investigations of the motorway alignment in the Šentvid tunnel area

Uporaba seizmične tomografije pri raziskavah AC trase na območju predora Šentvid

Janez Rošer[1], Robert Stopar[2], Andrej Gosar[1,3]

[1]University of Ljubljana, Faculty of Natural Sciences and Engineering, Aškerčeva cesta 12, SI-1000 Ljubljana, Slovenia; E-mail: janez.roser@ntf.uni-lj.si
[2]Geoinženiring d.o.o., Dimičeva ulica 14, SI-1000 Ljubljana, Slovenia; E-mail: robert.stopar@geo-inz.si
[3]Environmental Agency of the Republic of Slovenia, Dunajska cesta 47, SI-1000 Ljubljana, Slovenia; E-mail: andrej.gosar@gov.si

Received: December 19, 2007 **Accepted:** January 12, 2008

Abstract: The motorway tunnel Šentvid construction area has a very demanding geotechnical structure. On the basis of previous investigations, it was not possible to exactly define the best locations of merging caverns with ramp tunnels. That is why initially an exploration gallery has been constructed, in which different geological, geomechanical and geophysical investigations have been carried out. The goal of geophysical investigations was to obtain seismic parameters to define geomechanical rock mass characteristics in the region of planned merging caverns. Final solution is the velocity field of longitudinal and transversal seismic waves in the investigated region. Dynamic elastic moduli distribution of rock mass was also computed from seismic parameters. Seismic velocity fields and the distribution of dynamic elastic moduli well define areas of more compact rock mass.

Izvleček: Območje AC predora Šentvid je v geotehničnem smislu zelo zahtevno. Ker na podlagi predhodno izvršenih preiskav ni bilo mogoče natančno določiti lokacij kavern dveh priključnih predorov, je bil najprej izdelan raziskovalni rov, v katerem so bile izvedene različne geološke, geomehanske in geofizikalne raziskave. Cilj geofizikalnih raziskav je bil s pomočjo seizmičnih parametrov določiti geomehanske lastnosti posameznih kamnin v območjih načrtovanih priključnih kavern. Končni rezultat je hitrostno polje longitudinalnega in transverzalnega seizmičnega valovanja preiskovanega območja ter iz njiju izračunani dinamični elastični moduli hribine. Seizmična tomografija je dobro opredelila območja kompaktnejše kamnine, kar odražajo tako hitrosti longitudinalnega in transverzalnega valovanja kot tudi dinamični elastični moduli.

Review paper

Key words: geophysics, seismic tomography, Šentvid tunnel, dynamic elastic moduli
Ključne besede: geofizika, seizmična tomografija, predor Šentvid, dinamični elastični moduli

Introduction

The Šentvid tunnel is part of the motorway bypass of Ljubljana, section Šentvid – Koseze, which connects Ljubljana with Gorenjska motorway part. There were several attempts to establish motorway bypass in the past years, but all the suggested solutions were postponed because of their pretentiousness. Due to the unbearable traffic situation the investigations for tunnel construction finally commenced in 1999.

The twin-tube tunnel system Šentvid is divided into four units (Figure 1): two lane tunnel, ramp tunnels, merging caverns and three lane tunnel. The length of all tubes is approximately 3000 m and excavation profiles vary from 81 m^2 in ramp tunnels to 300 m^2 in merging caverns (Žigon et al., 2004). Due to outstanding dimensions of planning caverns and variable geological conditions, additional investigations were required to exactly define locations of the merging caverns. To satisfy all the requests an exploration gallery has been constructed (Figure 1).

Additional geophysical investigations were performed in several stages. In October 2004 the surface seismic refraction profiling was performed as the starting point for further seismic investigation activities. After the construction of the exploration gallery had finished in 2005, the seismic investigations between the surface, the exploration gallery and the boreholes were performed. The scope of the survey was characterization of the geotechnical conditions in the motorway tunnel Šentvid

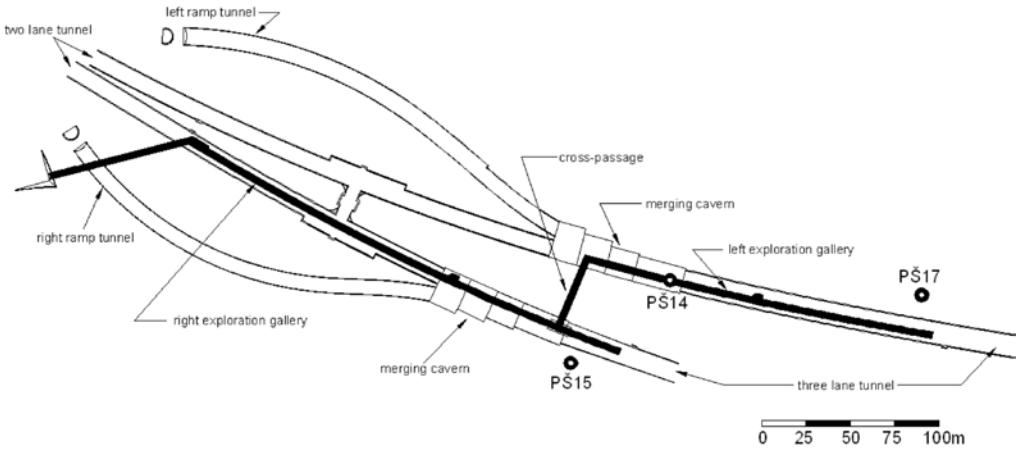

Figure 1. Alignment of the Šentvid tunnel and the exploration gallery
Slika 1. Trasa predora Šentvid in raziskovalnega rova

Table 1. Geomechanical parameters of Permian and Carboniferous layers
Tabela 1. Geomehanski parametri permokarbonskih plasti

Geomechanical parameters	*Layers of dark grey siltstone and clayed shalestone*	*Layers of light grey sandstone and dark grey micaceous siltstone*	*Tectonic clay and breccia*
RMR	class IV (35 points)	class III (42 points)	class V (< 20 points)
σ_c [*MP*a]	1.00	2.50 – 3.30	0.04 – 0.06
φ [°]	25 – 28	27 – 30	18 – 22
φ_{rez} [°]	22 – 25	24 – 27	15 – 19
c [*MP*a]	0.40	0.36 – 0.46	0.00
v [/]	0.26 – 0.27	0.25 – 0.26	0.29 – 0.31
E [*GP*a]	1.70 – 3.10	2.10 – 4.10	0.11

construction area. The goal of geophysical investigation activities was to use seismic parameters to define geomechanical rock mass characteristics in the region of planned merging caverns.

Geological conditions

The Šentvid tunnel alignment passes through Permian and Carboniferous sediments that include sandstone, siltstone and claystone, which are disintegrated from surface to about 30 m deep. In the tunnel area siltstone is prevalent. The region has undergone intense tectonic deformations, presumably during several deformation phases (Čadež et al., 2004). Tectonised zones consist of shalestone and highly tectonised clay.

Rock masses were characterized in terms of RMR (Rock Mass Rating). The following parameters for each different rock type were determined in laboratory: σ_c – uniaxial compressive strength of rock mass, E – modulus of elasticity, φ – angle of internal friction, φ_{rez} – residual friction angle, c – cohesion and v – Poisson's ratio (Fifer Bizjak et al., 2003). Geomechanical parameters are summarized in Table 1.

The lithological layers are generally sheared parallel to their schistosity. Fault gouge and fault breccias of all lithologies occur in association with faults and shear planes. The lateral continuity of the lithological layers is inconsistent due to frequent displacements along intersecting faults (Čadež et al., 2004).

Hydrogeological conditions in tunnel area are suitable and are classified as poorly permeable and small groundwater extractions (from 0.1 to 1.0 l/s per m of tunnel tube) are expected (Brenčič, 2000). In the tunnel area two hydrogeological units were defined: weathered and disintegrated rock in portal area and the interior rock mass. Both units differ in permeability and porosity.

FIELD INVESTIGATIONS

First phase investigations for Šentvid tunnel commenced in 1991. Later additional investigations began in 1999. In December 1999 the tunnel region was geologically and hydrogeologically mapped. In this phase five structural and nine geomechanical boreholes were drilled, which were all geologically monitored and cored. In boreholes seismic down-hole surveys, presiometric tests, SPT and slug tests were performed. Laboratory investigations of the mineralogical and geomechanical properties of characteristic rock samples were also done.

In October 2004 surface seismic refraction investigations started. On the basis of those results further geophysical investigations were planned. When the construction of the exploration gallery was finished at the beginning of 2005, geophysical measurements in the exploration gallery and between gallery, surface and boreholes were performed. Seismic investigations included surface refraction measurements along the tunnel alignment (10 linear arrays), tomography between the exploration gallery and the surface (5 linear arrays), tomography between the exploration gallery and the boreholes (2 linear arrays) and tomography between the right and left gallery (2 linear arrays).

SEISMIC TOMOGRAPHY

The mathematical basis for tomographic imaging was laid down by Johann Radon already in 1917. He showed that a form of an object could be obtained from its cross-sectional images. Due to computing power progress the tomographic method became very useful in astronomy, followed by great success in medicine and also in geophysics. The main restrain in geophysical tomography is that geometric factors are less determinable and that the investigation plain is mostly accessible only from two directions. Seismic tomography is used to image the interior of the Earth, for determining the elastic properties of the rock masses involved in geotechnical engineering and is particularly suitable for detecting and characterizing local structures, such as faults, fractures, cavities and other discontinuities.

For processing of tomographic data, the investigated area is divided into square grid, where cell dimensions depend on the seismic ray coverage (Figure 2). It is essential for a successful solution that every cell is intersected by multiple rays from different angles.

Travel time of the seismic ray between the source and the receiver is equal to the sum of travel times through every single cell. Consider that the source of seismic wave motion is in point *M (x, y)* and the receiver (geophone) is in point *N (x, y)*. Travel time of the signal is then written as (Figure 2):

$$t_{M,N} = \int_{L_{M,N}} \frac{1}{v(x,y)} ds$$

After discretisation:

$$T_{M,N} = \sum_i \sum_j \frac{1}{v_{i,j}} \cdot \Delta S_{i,j\,M,N}$$

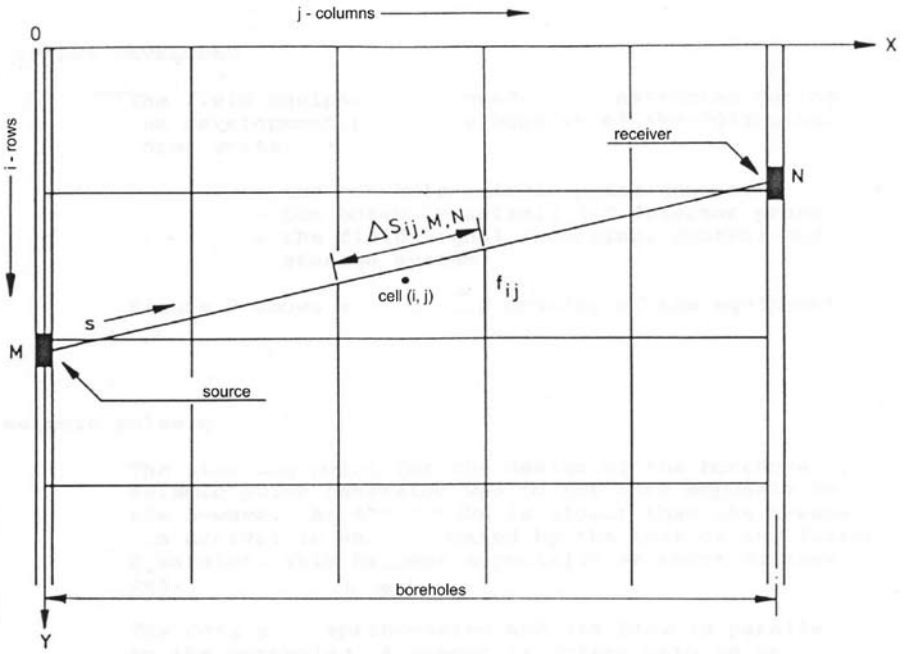

Figure 2. Velocity field in matrix form (Cosma et al., 1984)
Slika 2. Slika hitrostnega polja v matrični obliki (Cosma et al., 1984)

Tomographic inversion

By the tomographic inversion, the information obtained from field measurements is transformed to a model of the structure of the rock. Tomographic data sets often consist of many measurements. The result is that matrices can be large, sparse, and difficult to invert directly. A variety of computational methods have been developed to implement matrix inversions, such as generalized simulated annealing algorithm (SeisOpt, 2002) and simultaneous iterative reconstruction technique – SIRT (Jackson and Tweeton, 1994), which are both iterative solvers. These two methods were used to reconstruct the seismic velocity models in Šentvid tunnel tomography.

The generalized simulated annealing algorithm performs repeated forward modelling, where new models are conditionally accepted or rejected based on a probability criterion. This criterion allows the algorithm to escape from non-unique, local, travel-time minima to achieve a unique, globally optimized model of subsurface velocity structure (SeisOpt, 2002).

Another processing was performed by using the inversion algorithm based on the SIRT method. It updates an initial model through repeated cycles of forward travel time computation. Then the curved-ray inversion was performed. In the curved-ray tomography inversions the starting velocity model plays a crucial role, because the routine can be trapped in local minima misidentifying the global minimum solution (Dines and Lytle, 1979).

Seismic data acquisition

First we performed seismic refraction survey on the surface. Above the right exploration gallery there were 6 geophone arrays and above the left exploration gallery 4 arrays. Every array is composed of 24 geophones which record the seismic waves. Distance between receivers (4.5 Hz geophones) was 4 m. Three 24-channel digital seismographs with sample rate of 0.1 ms were used. The main purpose of refraction survey was to establish a reasonable starting model for tomography between the exploration gallery and the surface. The propagation of longitudinal (P) waves as well as transversal (S) waves was measured with all surface arrays. Because of a different kind of seismic noise (particularly traffic) and large source-receiver distances, a more powerful source was needed. Therefore explosive was used as a seismic source. It was placed in approximately 1 m deep boreholes spreading along the seismic profile. In this manner we successfully acquired refraction data from a depth of up to 50 m (Stopar, 2005). As a source of transversal wave motion we used a sledgehammer and specially designed wooden plank.

The same shot-points as for surface refraction were then used also for tomographic survey between the surface and the exploration gallery. Geophones were installed in the ceiling of the exploration gallery as shown in Figure 3. Seismic profile in the right exploration gallery consists of three linear arrays (72 geophones) and in the left exploration gallery of two arrays (48 geophones). The distance between geophones was also 4 m.

Figure 3. Vertical and horizontal geophone mounted on the ceiling of exploration gallery
Slika 3. Vertikalni in horizontalni geofon pritrjena na stropu raziskovalnega rova

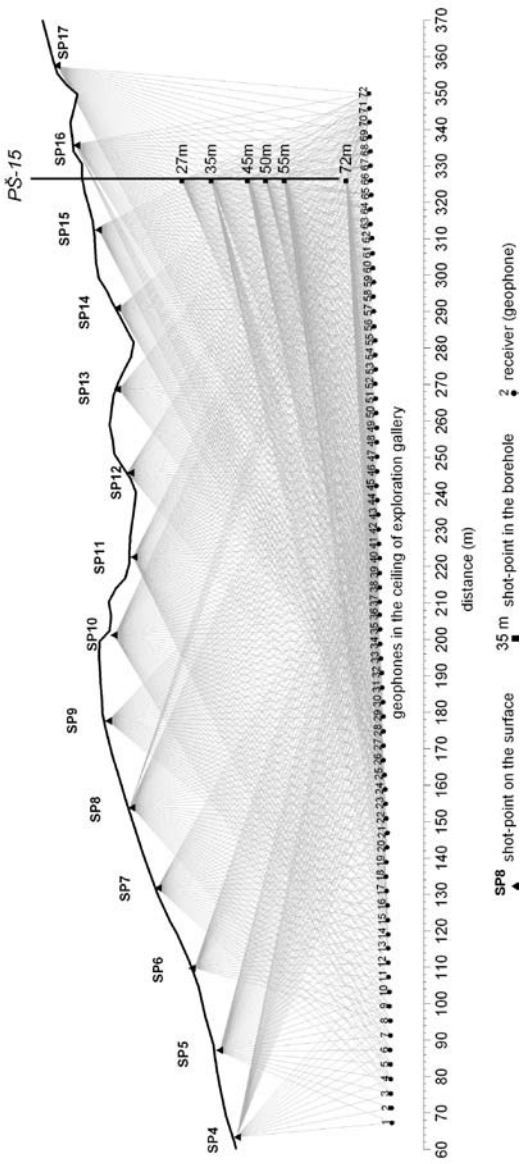

Figure 4. Tomography ray-density coverage for seismic rays between the right exploration gallery, the surface and the borehole PŠ-15
Slika 4. Gostota seizmičnih žarkov pri tomografiji med desnim rovom, površino in vrtino PŠ-15

Tomography was performed also between the right and the left exploration galleries. Geophones were located in the left gallery and the shot-points in a short section of the right exploration gallery and cross-passage (Figure 10). For the shot-points we drilled shallow boreholes (approximately 1 m) in which we inserted explosive.

To improve tomographic velocity fields in the lateral direction, tomography between boreholes and the exploration gallery was also conducted. The geophones were in the same locations in the ceiling as for tomography between the exploration gallery and the surface. Shot-points locations for tomography in the right exploration gallery were inside the borehole PŠ-15. The borehole PŠ-15 was 72 m deep. The shot-points in this borehole were at depths of 72 m, 55 m, 50 m, 45 m, 35 m and 27 m. The shot-points locations for tomography between the left exploration gallery and the boreholes PŠ-14 and PŠ-17 were in the borehole PŠ-17 at depths of 83 m, 78 m, 66 m, 53 m, 43 m, 33 m and 23 m. In the borehole PŠ-14 an obstruction occurred so that it was only possible to reach a depth of 50 m. Therefore the shot-points in PŠ-14 were at depths of 50 m, 40 m, 30 m and 25 m. Figure 4 represents tomography ray-density coverage for seismic rays between the right exploration gallery, the surface and the borehole PŠ-15. The boreholes PŠ-15 and PŠ-17 were out of the exploration gallery alignment for 15 m and 17 m, respectively (Figure 1). Thus corrections of the measured travel times were made.

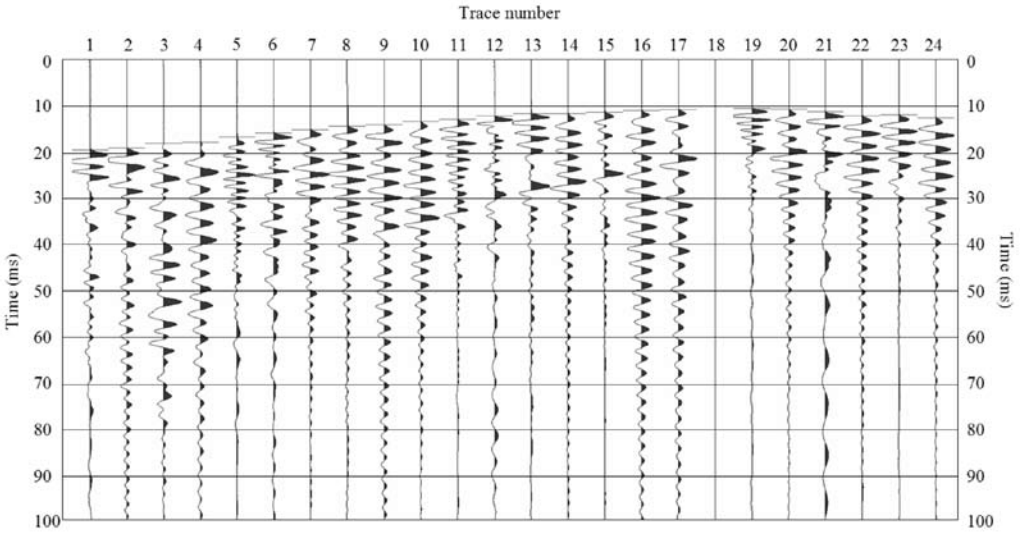

Figure 5. A representative seismic record with first arrivals picks obtained with explosive source on the surface and receivers in the exploration gallery
Slika 5. Značilen seizmični posnetek s prvimi prihodi seizmičnega signala pridobljen s proženjem eksploziva na površini in sprejemniki v raziskovalnem rovu

SEISMIC DATA ANALYSIS AND MODELLING

A total of 10176 travel times were recorded. Figure 5 shows a representative example of seismic records with corresponding picks of first arrivals of seismic waves, obtained with seismic tomography between the exploration gallery and the surface.

Initial data processing involved tomographic inversion based on a nonlinear optimization method using a generalized simulated annealing algorithm. The preliminary velocity data from the surface refraction seismic, interval velocities from the boreholes PŠ-14, PŠ-15 and PŠ-17 and the lithological data were used as constraints in the starting model. The final velocity model of the P waves acquired from tomography data between the surface, the right exploration gallery and the borehole PŠ-15 with 17901 nodes (81 by 221) and cell dimensions of about 1.5 m in both directions, is shown in Figure 6a. For seismic tomography of the S waves between the surface and the right exploration gallery, the tomographic calculations were carried out on a regular rectangular grid that occupied an area of about 330 m (horizontal) by 100 m (vertical), with 588 nodes (14 by 42) spaced at intervals of about 8 m in both directions (Figure 7).

Next, a more detailed processing by the use of the inversion algorithm based on the SIRT was performed. For seismic P-wave tomography between the surface, the right exploration gallery and the borehole PŠ-15 the tomographic calculations were carried out on a regular rectangular grid that occupied an area of about 300 m (horizontal) by 100 m (vertical), with 1220 nodes (20 by

61) spaced at intervals of about 5 m in both directions (Figure 6b). Figure 8 represents the final velocity model of the P waves acquired from tomography data between the surface, the left exploration gallery and the boreholes PŠ-14 and PŠ-17. The model consists of 700 nodes (25 by 28) spaced at intervals of about 7 m and 6 m in the *x* and *y* directions, respectively. In order to build a reasonable initial model for the curved-ray inversion, we started by inverting the travel time data with a straight-ray approximation using an initial velocity model obtained from the surface refraction data. A smoothed version of the updated model, obtained after 16 straight-ray iterations, was then used as a starting model for the successive curved-ray iterations. Before running new iterations, however, several explicit global and node constraints were incorporated into the model. Global constraints were imposed specifying the maximum and minimum allowable velocities, which equal to 6000 and 340 m/s (the P-wave velocity in the air), respectively. Node constraints, which force the solution to match known boundary values, were applied with a fuzzy logic approach (Jackson and Tweeton, 1994) using measured specimen velocities and other supplemental site information. Constraining the grid node is mainly where low ray-coverage imposed by source-to-receiver geometry, improved mathematical resolution by reducing the ill-conditioning of the inversion. For seismic tomography of the S waves between the surface and the left exploration gallery the tomographic calculations based on the SIRT technique was also performed. Due to a bad signal-to-noise ratio in the S wave data we had to use a smaller amount of data. That is why the model consists of 121 nodes and the cell dimensions are approximately 28 by 10 m (Figure 9). The tomographic calculations of the P waves data between the right and the left exploration gallery were carried out on a regular rectangular grid with 450 nodes (45 by 10) spaced at intervals of about 6.7 m and 5.5 m in *x* and *y* directions, respectively (Figure 10).

From the relation between the longitudinal and the transversal wave velocity, the dynamic elastic moduli were calculated. For the calculations we also needed the rock density data. The data were obtained from observations, laboratory and in situ measurements and are shown in Table 2 (Likar and Čadež, 2006). Calculations were based on a regular rectangular grid that occupied an area of about 340 m (horizontal) by 110 m (vertical), with 588 nodes (42 by 14) spaced at intervals of about 8 m in both directions. Rock density distribution inside the grid was determined with linear interpolation based on the range of wave velocity inside individual cells. We consider that higher seismic velocity corresponds to higher rock density and vice versa.

Results and discussion

Tomography between the right exploration gallery, the surface and the borehole PŠ-15

With the tomography between the right exploration gallery, the surface and the borehole PŠ-15 we acquired the exact data above the right tube of the Šentvid tunnel (Figure 6). From the result of modelling based on a nonlinear optimization method a low P velocity zone (velocities under 3000

Table 2. Rock density in the Šentvid tunnel area
Tabela 2. Gostota kamnin na območju predora Šentvid

Lithology	φ (g/cm^3)
Intercalations of meta-sandstone and meta-siltstone, meta-sandstone typically prevailing	2.65
Meta-siltstone with meta-sandstone layers/lenses, locally with slate layers	2.55
Slate, locally with meta-sandstone/ meta-siltstone layers	2.45
Fault breccia, fault gouge	2.30

m/s), which extends from the surface to the depth of about 30 m and indicates disintegrated rock, may be distinguished (Figure 6a). This low velocity zone is thicker on the side adjacent to the Celovška street, where parts of highly tectonised materials (probably shaly claystone) are anticipated. The second zone, characterized by P-wave velocities over 4000 m/s at distances of about 220 to 340 m, represents a more compact rock mass. With the use of the inversion algorithm based on the SIRT we acquired a more detailed P-wave distribution (Figure 6b). Up to distance of about 120 m we have disintegrated material, which resulting in low velocity zone. From that distance further a higher velocities are present, which corresponds to compact rock mass, presumably sandstone. In the vicinity of the shot-points on the surface are, due to higher resolution, noticeable abnormal areas with P-wave velocity around 3000 m/s. Individual curved shapes may indicate some geological structures, especially fault zones and incidental lithological layers. Low velocity zone in the right gallery, from 120 to 150 m, indicates highly tectonised zone. In general, the more compact rock masses correspond to P velocities of about 4000 m/s.

We obtained similar results from a tomographic S waves velocity image (Figure 7). Zone of the compact rock (S velocity over 1500 m/s) coincides with the results obtained from the tomographic P waves velocity image between the right exploration gallery, the surface and the borehole PŠ-15. Due to difference in cell dimensions between the S wave velocity model (cell size 8 by 8 m) and the P wave velocity model (cell size 1.5 by 1.5 m), the values of S wave velocity above the right exploration gallery are less reliable. From those models we can deduce that rock materials above the right tunnel tube is mostly tectonised, a minor zone of a compact rock is only in the lower right part of the tomogram, at distances of about 200 m to 320 m.

Tomography between the left exploration gallery, the surface and the boreholes PŠ-14 and PŠ-17

Figure 8 presents the result of the tomography between the left exploration gallery, the surface and the boreholes PŠ-14 and PŠ-17. As expected, lower P wave velocities (lower than 2000 m/s) are on the surface, where soil and weathered rock are present. With depth the velocity increases and in the central part of the tomogram, around elevation of 370 m, it exceeds 4000 m/s. This material corresponds to seismic compact rock mass. Relatively low seismic velocities (P velocity under 3500 m/s) appear at the beginning of the left exploration gallery, i.e. up to the distance of 140 m. This corresponds to a more tectonised rock, but also indicates a fault zone. At a distance of about 180 m in the left gal-

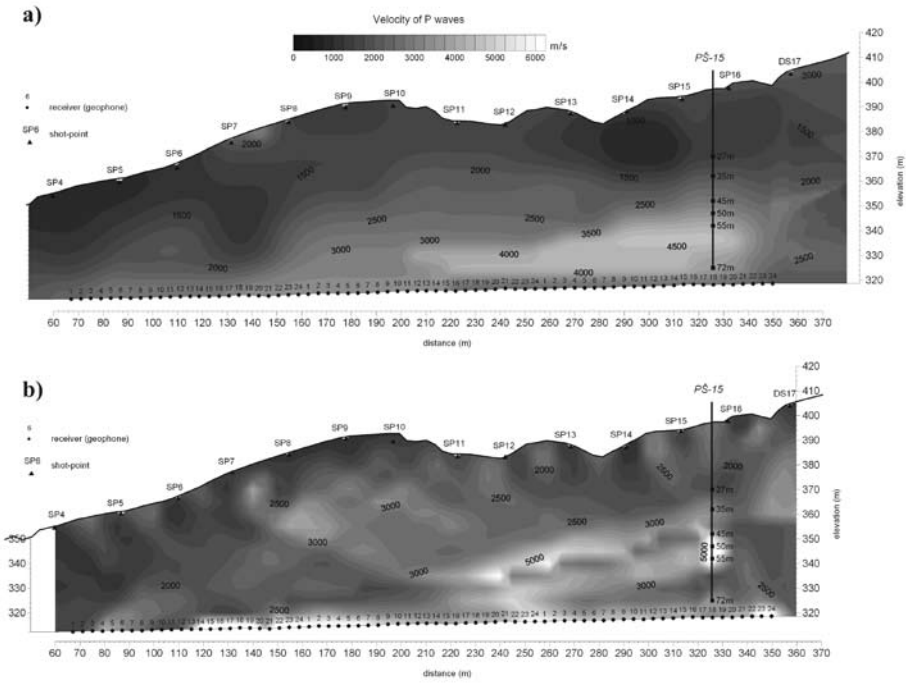

Figure 6. Tomographic P waves velocity image between the right exploration gallery, the surface and the borehole PŠ-15: a) nonlinear optimization method, b) SIRT method

Slika 6. Slika hitrosti P valov pridobljenih s tomografijo med desnim raziskovalnim rovom, površino in vrtino PŠ-15: a) nelinearna optimizacijska metoda, b) SIRT metoda

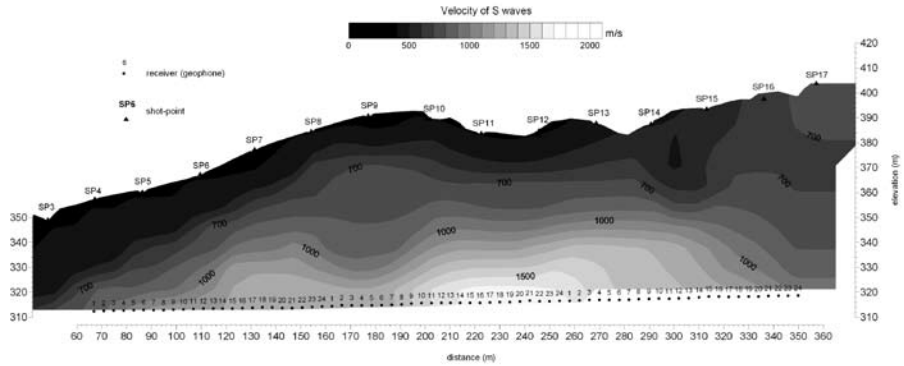

Figure 7. Tomographic S waves velocity image between the right exploration gallery, the surface and the borehole PŠ-15 (nonlinear optimization method)

Slika 7. Slika hitrosti S valov pridobljenih s tomografijo med desnim raziskovalnim rovom, površino in vrtino PŠ-15 (nelinearna optimizacijska metoda)

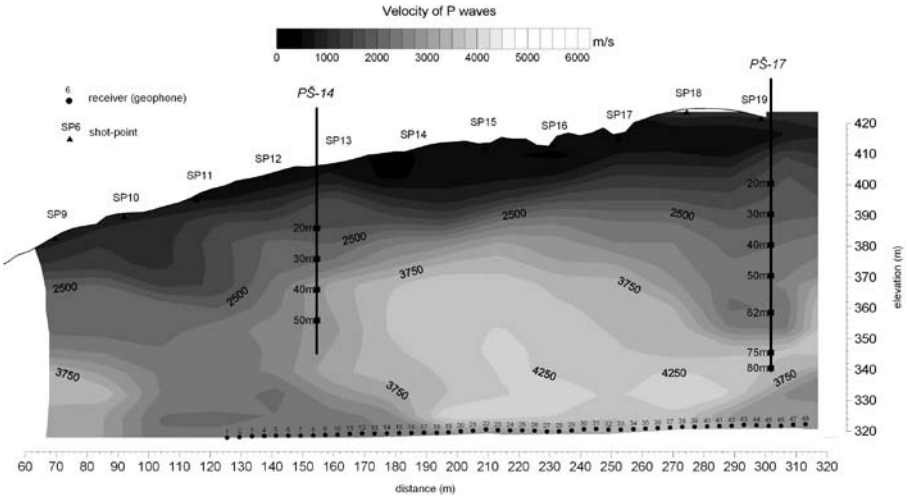

Figure 8. Tomographic P waves velocity image between the left exploration gallery, the surface and the boreholes PŠ-14 and PŠ-17 (SIRT)
Slika 8. Slika hitrosti P valov pridobljenih s tomografijo med levim raziskovalnim rovom, površino in vrtinama PŠ-14 in PŠ-17 (SIRT)

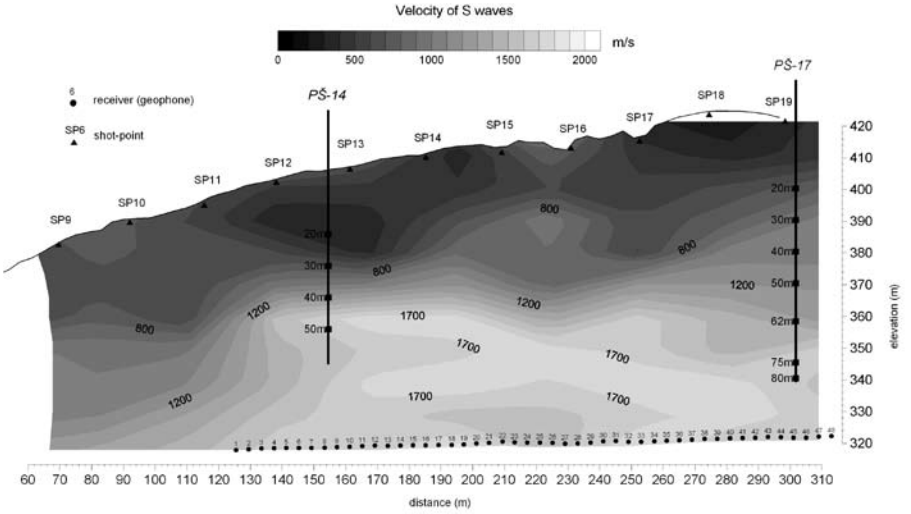

Figure 9. Tomographic S waves velocity image between the left exploration gallery, the surface and the boreholes PŠ-14 and PŠ-17 (SIRT)
Slika 9. Slika hitrosti S valov pridobljenih s tomografijo med levim raziskovalnim rovom, površino in vrtinama PŠ-14 in PŠ-17 (SIRT)

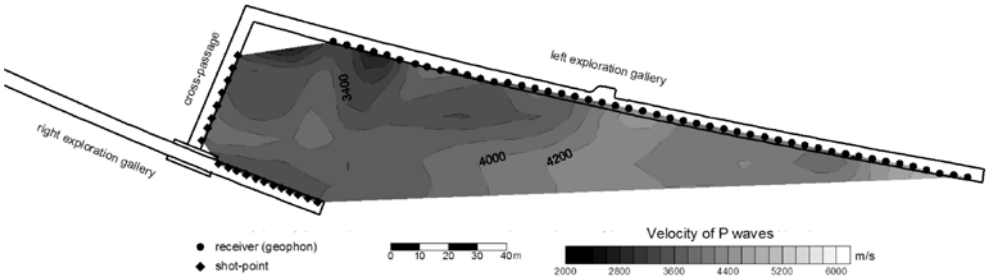

Figure 10. Tomographic P waves velocity image between the right and the left exploration gallery (SIRT)
Slika 10. Slika hitrosti P valov pridobljenih s tomografijo med desnim in levim raziskovalnim rovom (SIRT)

lery we find more favourable conditions. The P wave velocities over 4000 m/s correspond to a compact rock, most likely to sandstone. The overburden height in the left exploration gallery is higher than in the right exploration gallery. For that reason seismic data from tomography above the left exploration gallery did not have sufficient resolution to correctly image the low velocity zone at the beginning of the left gallery.

From the tomographic S waves velocity image (Figure 9) similar result was obtained. Because water does not influence propagation of the transversal waves, low velocity surface layers could be even thicker. Nevertheless, higher S velocities (above 1500 m/s) indicate more compact rock mass. In modelling of the S wave velocity field above the left exploration gallery only half the amount of data as for P waves velocities was used. Thus the S wave velocity image resolution is smaller than the resolution of the P wave velocity image (Stopar, 2005).

Tomography between the right and the left exploration gallery

The final velocity model of the P waves acquired from tomography data between the right and the left exploration galleries is shown in Figure 10. In the first 80 m from the cross-passage, the velocity model is rather reliable. From that point further the image of P wave velocity is unreliable, due to almost parallel seismic rays. At the start of the left exploration gallery a low velocity zone, with velocity varying from 3000 to 3500 m/s, was found. According to geological data acquired during the exploration gallery construction that low velocity zone correlates with highly tectonised claystone and siltstone. Velocity increases in the direction along the left exploration gallery, where one of the merging caverns is planned. Although that velocity is relatively high, the materials in this area are moderately tectonised. At tomography between the right and the left exploration galleries we do not have to deal with surface soil and weathered materials. Thus the P wave velocities are higher than the values

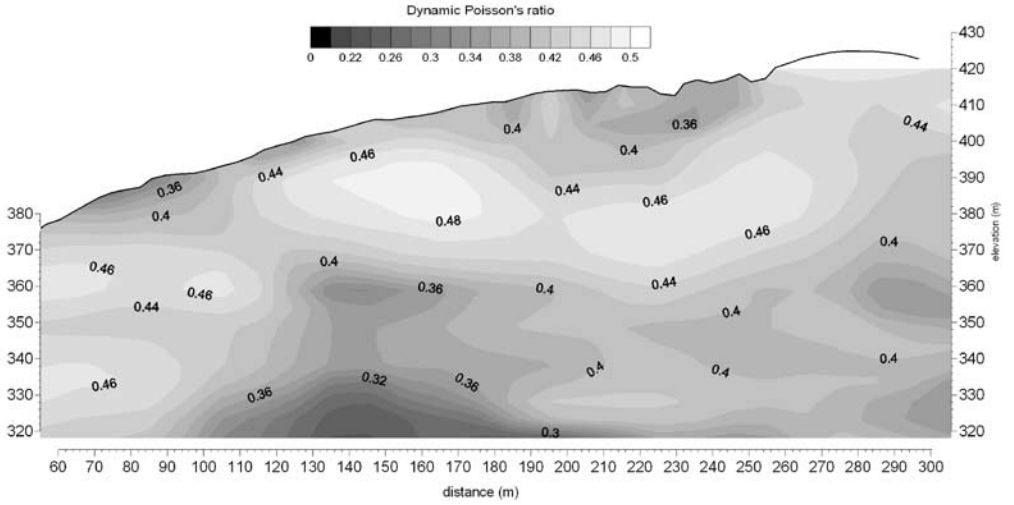

Figure 11. An example of obtained dynamic elastic moduli – values of dynamic Poisson's ratio above left exploration gallery
Slika 11. Primer pridobljenih dinamičnih elastičnih modulov – vrednosti dinamičnega Poissonovega količnika nad levim raziskovalnim rovom

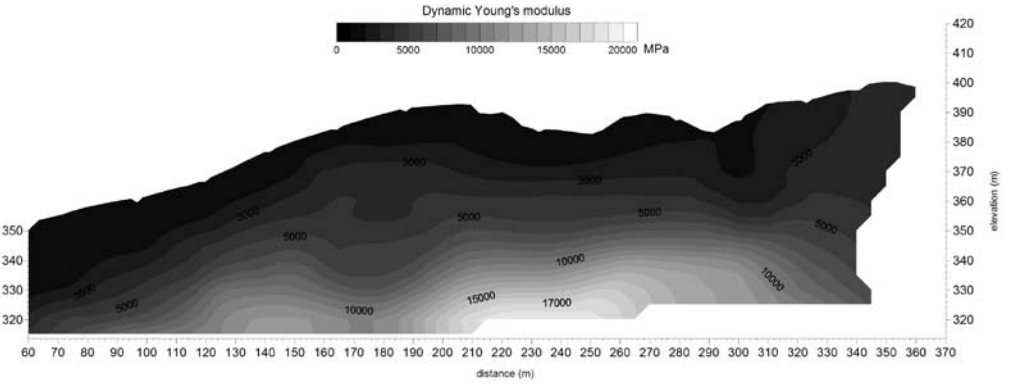

Figure 12. An example of obtained dynamic elastic moduli – values of dynamic Young's modulus above the right exploration gallery
Slika 12. Primer pridobljenih dinamičnih elastičnih modulov – vrednosti dinamičnega Youngovega modula nad desnim raziskovalnim rovom

obtained with tomography between the surface and the exploration gallery. Higher disintegration of material is also a consequence of the exploration gallery construction.

Seismic dynamic elastic moduli

We determined that values of dynamic Poisson's ratio vary from 0.24 to 0.48 (Figure 11). Higher values of dynamic Poisson's ratio near the surface are a consequence of saturated weathered and disintegrated material. The values of the dynamic Young's modulus vary from 1000 to 20000 MPa as shown in Figure 12. Compared to laboratory acquired Young's moduli for different rock types (Table 1), the calculated dynamic Young's moduli are one magnitude greater. The dynamic shear modulus varies from 200 to 7000 MPa and the dynamic bulk modulus varies from 100 to 40000 MPa. A larger anomaly appears along the right exploration gallery at distance of approximately 220 m, where values of the dynamic elastic moduli are higher. According to the seismic velocity data, the data from boreholes and other geological information, we can deduce that rock mass here is less tectonised.

Taking mutual relations between dynamic elastic moduli and P and S wave velocities into account, the similarity of geological structures in all the images is not surprising. The ratio between the static and dynamic elastic moduli depends on the type of material and is usually smaller than one. The real meaning of the dynamic elastic moduli is that we can use them to distinguish between geotechnically good and weak rock masses, because in contrast to laboratory measurements a larger volume of the material is taken into consideration.

Conclusions

The goal of geophysical investigations was to obtain seismic parameters to define geomechanical rock mass characteristics in the region of planned merging caverns. Final solutions are the P and S wave velocity fields with additional dynamic elastic moduli calculations. All the solutions well indicate areas of a more compact rock mass. The real value of acquired data is that it presents "in-situ" conditions along the tunnel alignment. Seismic measurements between the surface and the exploration gallery were, difficult to perform due to large distances, several communications, urban noise and construction works in the exploration gallery. In spite of all that, the seismic P wave propagation signal was of good quality, only the signal data of the S wave propagation was less satisfactory, especially those from the most distant shotpoints. The tomographic velocity models of the P waves present a satisfying complementary solution for locating merging caverns. The S wave velocity results of the tomography between the surface, the exploration gallery and the boreholes are not so good than the P wave velocity results. Reasons for that could be in a less accurate determination of the transversal waves arrivals, in a smaller amount of information due to worse signal-to-noise ratio and also because the variations of geomechanical parameters have a more significant effect on transversal than on longitudinal waves. Nevertheless the velocity fields of longi-

tudinal and transversal waves and the dynamic elastic moduli distribution well indicate areas of a more compact rock mass.

Povzetek

Uporaba seizmične tomografije pri raziskavah AC trase na območju predora Šentvid

Predmet geofizikalnih raziskav je bilo območje izgradnje predora Šentvid. Šentviški hrib bo avtocesta prečkala v obliki dveh ločenih predorskih cevi s priključnima cevema, poseg pa je zaradi neugodne geološke zgradbe zelo zahteven. Ker na podlagi predhodno izvršenih preiskav ni bilo mogoče natančno določiti lokacij priključnih kavern, je bil najprej izdelan raziskovalni rov, v katerem so bile izvedene različne geološke, geomehanske in geofizikalne raziskave. Cilj geofizikalnih raziskav je bil, s pomočjo seizmičnih parametrov, določiti geomehanske karakteristike posameznih kamnin v območjih načrtovanih priključnih kavern. Geofizikalne raziskave so vključevale površinsko seizmično refrakcijsko profiliranje in seizmično tomografijo med površino, vrtinami in raziskovalnim rovom.

Rezultati seizmičnih preiskav v in nad raziskovalnim rovom predora Šentvid odražajo predvsem mehanske lastnosti preiskovane kamnine v nadkritju predora. Vrednost pridobljenih podatkov je v tem, da predstavljajo "in-situ" podatek vzdolž zveznih profilov. Glede na to, da velik del vrednosti hitrosti longitudinalnega valovanja izvedenih raziskav seizmične tomografije dosega 3000 m/s in več, lahko govorimo o hribini. Izjema so površinske plasti, ki zlasti v smeri proti severnemu portalu dosegajo tudi debelino več deset metrov. Posamezne nižje hitrostne anomalije so posledica pretrte kamnine ali prelomnih con. Seizmične raziskave so dobro podale območja kompaktnejše kamnine, kar odražajo tako slike hitrosti longitudinalnega in transverzalnega valovanja kot tudi slike dinamičnih elastičnih modulov. Predvideni lokaciji priključnih kavern sta bili na osnovi dodatnih raziskav, med katere sodijo tudi geofizikalne, potrjeni.

References

Brenčič, M. (2000): *Hidrogeološko poročilo za predor Šentvid*. Geološki zavod Slovenije, Ljubljana, unpublished report, 45 p.

Cosma, C., Ihalainen, M., Korhonen, R. (1984): The Crosshole Seismic Method. *Report of phase II. of development programme*. Helsinki, 36 pp.

Čadež, F., Kleberger, J., Genser, W., Pöschl, I. (2004): Sentvid Motorway Tunnel – Interim Results from Slovenia's Most Recent Exploration Gallery. *7. mednarodno posvetovanje o gradnji predorov in podzemnih prostorov, zbornik referatov*. Uredila: Kostiov, L. in Likar, J., Ljubljana: Društvo za podzemne in geotehnične konstrukcije in Univerza v Ljubljani, pp. 50-56.

Dines, K. A. and Lytle, J.R. (1979): Computerized Geophysical Tomography. *Proceedings of the IEEE*.; Vol. 67, No. 7, pp. 1065-1073.

Fifer Bizjak, K., Petkovšek, B., Petrica, R. (2003): Geološke in geomehanske raziskave za predor Šentvid. *Gradbeni vestnik*.; Vol. 52, pp. 15-21.

Jackson, M.J., Tweeton, D.R. (1994): MIGRATOM – Geophysical tomography using wavefront migration and fuzzy constraints. *USBM Report of Investigation 9497*. United states department of the interior, Bureau of mines, 35 p.

Likar, J., Čadež, J. (2006): *Verification analysis of the stability of large underground caverns in the three-lane road tunnel Šentvid*. FLAC and Numerical Modeling in Geomechanics – 2006, proceedings of the 4th international FLAC symposium, Spain, pp 71 – 77.

SeisOpt@2d (2002): Ver. 3.0, *Seismic Refraction Tomography software copyright Optim, Inc.*, University of Nevada, Reno, Nevada.

Stopar, R. (2005): *Poročilo o geofizikalnih preiskavah na območju predora Šentvid (levi in desni raziskovalni rov)*. Geoinženiring d.o.o., Ljubljana, unpublished report, 16 p.

Žigon, A., Žibert, M. in Jemec, P. (2004): Projektiranje predorskega sistema Šentvid. *7. mednarodno posvetovanje o gradnji predorov in podzemnih prostorov, zbornik referatov.* Uredila: Kostiov, L. in Likar, J., Ljubljana: Društvo za podzemne in geotehnične konstrukcije in Univerza v Ljubljani, pp. 125-147.